



## Combined helium ion beam and nanoimprint lithography attains 4nm half-pitch dense patterns

Wen-Di Li, Wei Wu, and Richard Stanley Williams

Citation: *Journal of Vacuum Science & Technology B* **30**, 06F304 (2012); doi: 10.1116/1.4758768

View online: <http://dx.doi.org/10.1116/1.4758768>

View Table of Contents: <http://scitation.aip.org/content/avs/journal/jvstb/30/6?ver=pdfcov>

Published by the AVS: Science & Technology of Materials, Interfaces, and Processing

---

### Advertisement:



## Re-register for Table of Content Alerts

Create a profile.



Sign up today!



# Combined helium ion beam and nanoimprint lithography attains 4 nm half-pitch dense patterns

Wen-Di Li,<sup>a)</sup> Wei Wu,<sup>b)</sup> and Richard Stanley Williams<sup>c)</sup>  
*Cognitive System Lab, Hewlett-Packard Labs, Palo Alto, California 94304*

(Received 30 June 2012; accepted 24 September 2012; published 17 October 2012)

The authors demonstrated a promising technique that yielded single-digit nanometer features for nanotechnology research and possible future electronic circuit fabrication by combining high resolution helium ion beam patterning and nanoimprint lithography. They fabricated a series of line patterns with single-digit nanometer half-pitches by exposing a layer of hydrogen silsesquioxane (HSQ) resist with a scanning focused helium ion beam. The smallest half-pitch of clearly resolved line patterns was 4 nm. Using the HSQ patterns as a nanoimprint template, nanoscale patterns down to 4 nm half-pitch were transferred into nanoimprint resist through a UV-curable nanoimprint process. © 2012 American Vacuum Society. [<http://dx.doi.org/10.1116/1.4758768>]

## I. INTRODUCTION

After keeping pace with Moore's Law for more than four decades,<sup>1</sup> the semiconductor industry could be entering the sub-10 nm node size regime by the end of this decade. Thus, next-generation nanolithography technologies are facing unprecedented challenges. Scanning electron beam lithography (EBL), the current major workhorse of nanolithography, has set a patterning resolution record of 4.5 nm half-pitch lines.<sup>2</sup> Further improving the patterning resolution of EBL is likely limited by the resist development behavior,<sup>3</sup> while other factors, such as primary beam spot size, resist contrast, secondary electron broadening, etc., may also affect the resolution limit. In addition, strong proximity effect, which mainly arises from the backscattering of the primary electrons and substantial secondary electron generation, also brings challenges to the making of dense and complex patterns with sub-20 nm features.

In the recently introduced scanning helium ion microscope (HIM),<sup>4</sup> helium ions from a high-brightness source are focused at a small spot size and scanned over the sample for imaging and lithography.<sup>5–10</sup> In lithography applications, previous results have shown sub-10 nm half-pitch lines and dots patterned in hydrogen silsesquioxane (HSQ) by a scanning focused helium ion beam.<sup>5,6</sup> Though they are still short of the record resolution of EBL, focused helium ion beams have a number of advantages over electron beams. First, with a mass more than 7000 times greater than an electron, a helium ion is less diffractive due to a much shorter de Broglie wavelength. Therefore, smaller apertures (e.g.,  $<5 \mu\text{m}$ ) can be used in HIM to suppress the angular spread of the helium ion beam, hence reduce spherical aberration and beam spot size. The high brightness of the source in the Orion HIM ensures sufficient beam current even at smaller aperture, i.e., smaller beam spot size. Second, as illustrated in Fig. 1, helium ions have a smaller interaction volume with typical substrates (e.g., silicon) than electrons with similar energy. That results in a

higher surface sensitivity for imaging and a smaller proximity effect for lithography. An imaging resolution of 0.24 nm has been reported using a helium ion microscope.<sup>11</sup> With both smaller focus spot and smaller proximity effect, helium ion beam lithography (HIBL) has the potential to be a higher resolution process than EBL. However, as serial scanning beam lithography, it is also limited by low throughput and therefore high cost. Moreover, accumulation of helium atoms trapped in substrate materials can produce bubbles and voids, creating damage and defects in electronic circuits.<sup>12</sup> Thus, although HIBL has potential as a nanolithography tool for single-digit nanometer patterning, solutions for overcoming the low-throughput and substrate damage need to be developed.

Here we present a potential solution: combining HIBL with nanoimprint lithography (NIL), which is based on the mechanical deformation of a thermal- or UV-curable polymer resist by contacting with a template carrying surface relief patterns.<sup>13</sup> NIL is a high-throughput, low-cost patterning technology with molecular-scale resolution.<sup>14–16</sup> We used a scanning helium ion microscope as a patterning tool to make an imprint template and then transferred the features into a UV-curable resist through a UV nanoimprint process to combine the high resolution of HIBL with the high throughput of NIL. We achieved a patterning resolution of 4 nm half-pitch lines in HSQ resist using HIBL and also transferred the 4 nm half-pitch lines in UV-curable resist through a NIL process using the HIBL-patterned template.

## II. EXPERIMENT PROCEDURE

We performed HIBL using a Carl Zeiss Orion Plus scanning HIM operated at 35 kV and equipped with a Raith ELPHY Multibeam pattern generator. In order to achieve optimal beam quality, we carefully conditioned the helium ion microscope with a refreshed source and chose a  $5 \mu\text{m}$  aperture to achieve a beam current of about 1 pA. The gun temperature during our writing was stable at 72 K, ensuring minimal thermal drift of the electro-optic elements and maintaining constant focus and astigmatism calibration. The helium pressure in the gun was  $5 \times 10^{-6}$  Torr, and we used a working distance of approximately 7.5 mm for all the writing. The system was housed in a quiet room to isolate and

<sup>a)</sup>Present address: Department of Mechanical Engineering, University of Hong Kong, Pokfulam, Hong Kong; electronic mail: liwd@hku.hk

<sup>b)</sup>Present address: Department of Electrical Engineering, University of Southern California, Los Angeles, CA 90089; electronic mail: wu.w@usc.edu

<sup>c)</sup>Electronic mail: stan.williams@hp.com

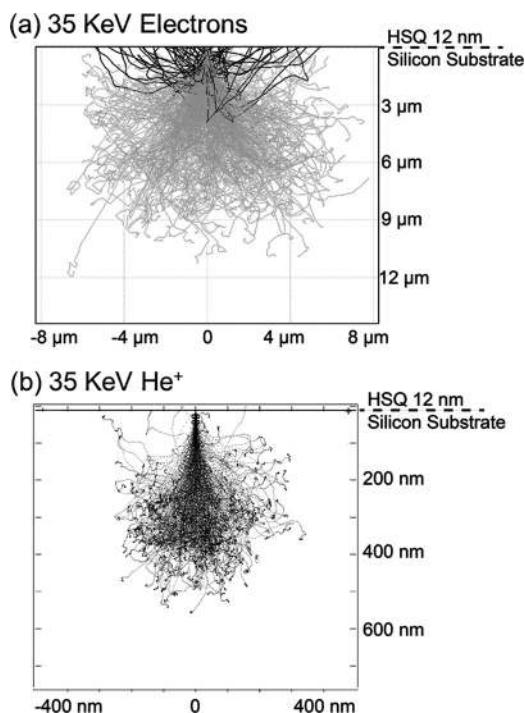


FIG. 1. Monte Carlo trajectory simulation of (a) 35 keV electrons and (b) 35 keV helium ions incident onto a silicon substrate with a 12 nm HSQ resist overlayer. In (a), the dark traces represent backscattered electron trajectories that exit the sample through the resist overlayer. Note the  $\sim 20\times$  difference in length scale between the two figures. The much smaller interaction volume of He ion with typical substrates (e.g., silicon) results in a higher surface sensitivity in imaging and a smaller proximity effect for lithography.

suppress environmental noise and electromagnetic interference in order to obtain subnanometer beam resolution.

A pattern generator was used to steer the helium ion beam for writing arbitrary patterns. The ELPHY system has a 16-bit DAC to scan 65 536 stepping points across the writing field, resulting in a minimum step size of 2 nm at a 100- $\mu\text{m}$  writing field and 0.2 nm at a 10- $\mu\text{m}$  writing field. In order to achieve accurate patterning for sub-5 nm features, we used the 10  $\mu\text{m}$  writing field in our experiments. At each stepping point, the minimum dwell time was 50 ns, and the dwell time can be varied for a broad dose range.

The negative-tone resist employed here for HIBL was HSQ with a recently introduced saline development process.<sup>17</sup> HSQ has been widely used in high-resolution EBL demonstrations, for example, 4.5-nm half-pitch lines,<sup>2</sup> and in previous HIBL work.<sup>5,6</sup> We directly used the HSQ pattern as a nanoimprint template without first transferring it into other conventional template materials such as silicon and silica. Fully crosslinked HSQ has a relatively high mechanical strength comparing with other carbon based polymer resists and has been previously demonstrated for direct nanoimprint process.<sup>18</sup> However, HSQ has a lower Young's modulus than typical hard template materials; therefore, the deformation and lifetime of a HSQ template may need further investigation. The HSQ resist used in our experiment was purchased from Dow Corning (XR-1541, 2%) and was further diluted with semiconductor-grade methyl isobutyl ketone (MIBK). The diluted HSQ resist was spin-coated to a

thickness of 12 nm, as measured by ellipsometry, onto a 1.5 cm  $\times$  1.5 cm silicon substrate, and the resist film was dried in air without baking. Before exposure, we made scratches near the center of the sample using a diamond scribe to help optimize the focus and stigmatism adjustment near the writing position and to locate the pattern for later imaging. After helium ion beam exposure, the resist was developed in a saline solution (1% NaOH and 4% NaCl in deionized water for 4 min) that has been shown to have a superior contrast for sub-10 nm features exposed by both electrons and helium ions. The resulting HSQ patterns were examined under a scanning electron microscope (SEM) (FEI XL30) operated at 20 kV and 6 mm working distance.

After inspection with the SEM, the resist pattern was treated in oxygen plasma briefly to clean the surface. Then, the sample was coated with a vapor-phase self-assembled monolayer<sup>19</sup> of mold release agent (trichloro(1H, 1H, 2H, 2H-perfluorooctyl)silane) in a modified atomic layer deposition system and used as a template for UV-curable NIL in a custom-made nanoimprinter.<sup>14</sup> The substrate to be imprinted was transparent glass with a 4 nm thick titanium film to decrease charging during ion and electron beam imaging. The substrate was spin-coated with a 30 nm thick PMMA film as the transfer layer, followed by a 100 nm thick UV resist, composed of a low viscosity acrylated poly(dimethylsiloxane), a multifunctional acrylate cross-linker, and a free radical

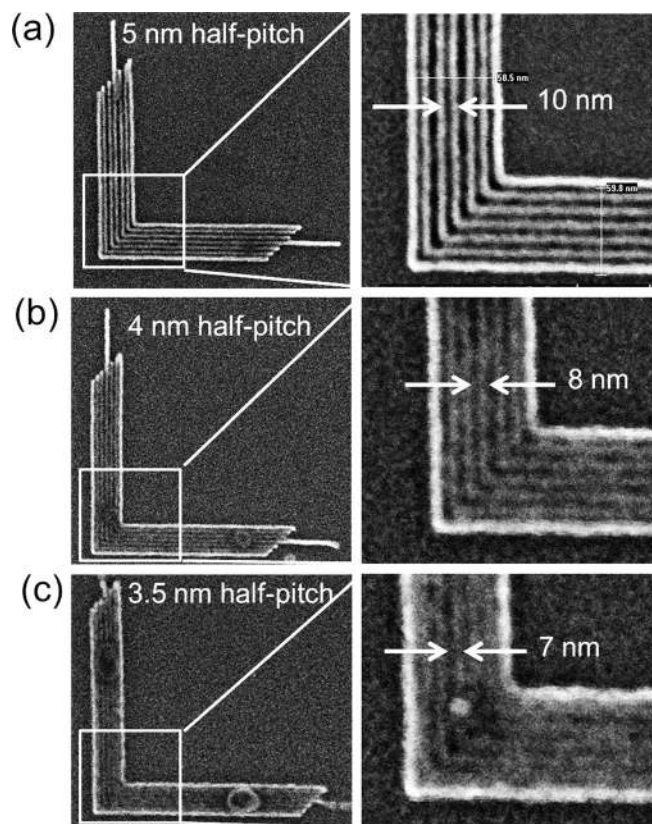


FIG. 2. SEM images of (a) 5 nm, (b) 4 nm, and (c) 3.5 nm half-pitch nested L's formed by helium ion beam lithography in an HSQ layer that was subsequently developed to remove unexposed resist. Five nanometers and 4 nm half-pitch patterns were clearly resolved. Although the 3.5 nm half-pitch patterns were not completely resolved, there were regions in which individual lines are distinct.

initiator.<sup>20</sup> The HSQ template was pressed into the resist film, which was cured with UV light through the substrate. After removing the template, the imprinted sample had a thin metal layer deposited on it to prevent charging during imaging in the SEM.

### III. RESULTS AND DISCUSSION

The pattern we used to test our lithographic resolution was a nested “L,” which consisted of right-angle line segments (Fig. 2) with half-pitches ranging from 3 to 24 nm. The L’s were single pixel lines and the arrays were patterned with ion doses ranging from 10 to 200 pC/cm. The  $10\ \mu\text{m} \times 10\ \mu\text{m}$  writing field was used to provide a pixel step size of 0.2 nm. Figure 2 shows SEM images taken of nested L’s with half-pitches of 5, 4, and 3.5 nm. The 5 nm half-pitch lines are clearly resolved with little resist residue observed between lines. The 4 nm half-pitch lines are also resolvable with clear contrast, although resist residues can be observed between lines. The residues may be a result of self-limiting

development, particularly for very narrow trenches, due to surface charge screening on the HSQ surface.<sup>2,17</sup> Comparing with the 5 and 4 nm half-pitch lines, the 3.5 nm half-pitch patterns are not well resolved, although there are regions in which individual lines are distinct. The optimal dose for the 5 and 4 nm half-pitch single pixel lines were found to be approximately 110 and 90 pC/cm, respectively. Many factors can limit the achievable resolution in our sub-10 nm helium ion beam patterning. One major limiting factor is the resist development process, including self-stopping development due to surface charge screening, capillary force induced pattern deformation for high-aspect-ratio resist structures, etc. Although thinner HSQ resist may be beneficial for mitigating the challenges in resist development, further reducing HSQ thickness to below 10 nm will bring more difficulty in our subsequent nanoimprint process as the developed HSQ is directly used as the nanoimprint template. Another limiting factor for further improving the resolution lies in the interaction between the incident helium ions and the HSQ resist. Many factors, including nonzero primary beam spot size, secondary electron broadening, forward scattering of primary helium ions, etc., can expand the point spread function (PSF) or the distribution of deposited energy in resist, limiting further increase of the patterning resolution. However, our result has shown that HIBL can achieve comparable or superior patterning resolution than EBL. Imaging equipments also limit our capability to accurately characterize the quality of the patterns at sub-5 nm sizes, which approach the imaging resolution limit of our SEM. The environmental vibrations in our SEM room further limited our imaging resolution. Ideally, high-resolution transmission electron microscope should be used to more accurately and reliably characterize the patterning quality at sub-5 nm scale.

After we cleaned and treated the HIBL patterned samples with mold release agent, they were used as nanoimprint templates. The imprinted samples were coated with 2 nm thick platinum to enhance the electrical conductivity and signal contrast during SEM imaging. Inspection under the SEM verified that nested L’s with half-pitch down to 4 nm were resolvable in the UV-curable resist. Figure 3 shows typical SEM images collected from the imprinted samples with mirrored

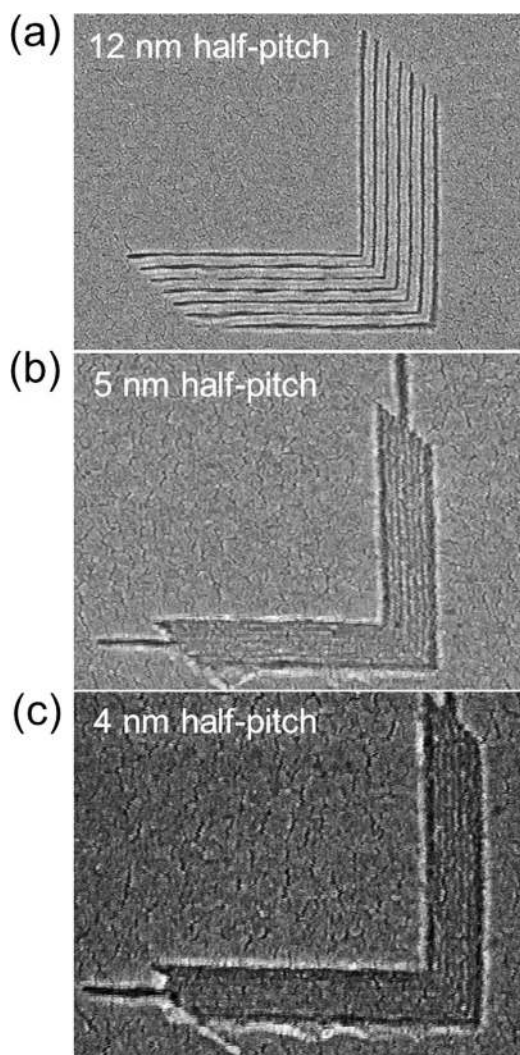


FIG. 3. SEM images of nanoimprint results using the HIBL written template to create depressions in a layer of imprint resist. Feature half pitch: (a) 12 nm, (b) 5 nm, and (c) 4 nm. The samples have been coated with a thin Pt film to minimize charging. Because of the deposited metal, the samples have a grainy appearance. Four nanometers half-pitch patterns were resolved.

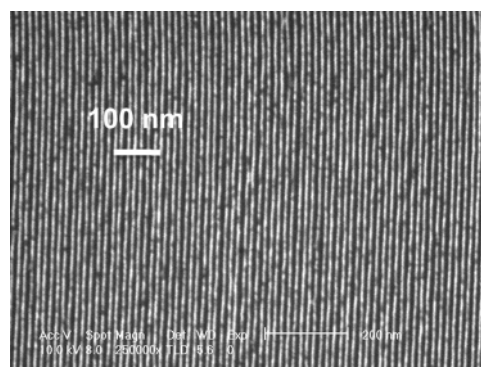


FIG. 4. SEM image of a square micron area of dense 8 nm half-pitch lines patterned on 12 nm thick HSQ resist using HIBL exposure followed by development, which illustrates the fact that the cumulative proximity effect over the entire pattern area does not wash out the lines.

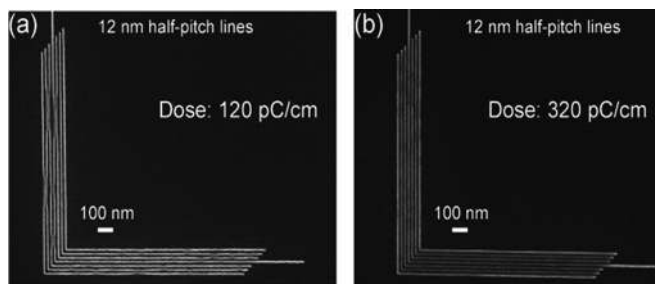


Fig. 5. SEM pictures of 12 nm half-pitch nested L's patterned in HSQ resist by HIBL at doses of (a) 120 pC/cm and (b) 320 pC/cm, to illustrate the broad dose window.

nested L's at half-pitches of 12, 5, and 4 nm. The depth of the imprinted lines is limited by the height of the HSQ template patterns. Because of the deposited metal, the samples have a grainy appearance. Although 2 nm NIL resolution has been demonstrated using isolated random carbon nanotubes as templates,<sup>15</sup> our result of dense patterns of 4 and 5 nm half-pitch lines have better resolution than previously reported nanoimprinted patterns with designed templates.<sup>14</sup>

The 4 nm HSQ line pattern demonstrated in this work provides the experimental evidence that focused helium ion beam can achieve higher patterning resolution than that achieved by a focused electron beam,<sup>2</sup> which has been expected but not demonstrated before. The superior resolution of HIBL is due to both smaller beam spot size and less proximity effect. Figure 1 compares the simulated trajectories of 35 keV electrons and 35 keV helium ions after entering a silicon substrate coated with 12 nm thick HSQ as used in our work. The trajectories of electrons and helium ions were calculated by CASINO (Ref. 21) and TRIM,<sup>22</sup> respectively, both of which are Monte Carlo simulation algorithms. The distance scale for the ion trajectories in Fig. 1(b) is a factor of  $\sim 20$  smaller than for the electron simulations in Fig. 1(a), illustrating the substantial difference in interaction volumes (nearly four orders of magnitude) for the two species. More importantly, a substantial fraction of backscattered electrons [dark traces in Fig. 1(a)], with a backscattering coefficient of 11.6%, spread out over a several micron radius around the incident electron beam and exit the sample back through the HSQ layer, while less than 1% helium ions backscatter into the resist layer after entering the substrate and spread over a much smaller area of only about 200 nm radius at the exit surface. As a result, the helium ion beam has much less proximity effect and a smaller point-spread function within the resist layer.<sup>23</sup> Experimentally, the significantly reduced proximity effect of HIBL results in the potential for patterning high-resolution features over a large area and with a large dose window. Due to proximity effect, the dose background from neighbor patterns reduces the dose contrast. That is especially severe when exposing sub-10 nm dense patterns over a large area using EBL. With HIBL, patterning of sub-10 nm features over a large area is much improved. Figure 4 shows an array of 8 nm half-pitch dense gratings over a  $1 \mu\text{m} \times 1 \mu\text{m}$  area, which we were not able to achieve using EBL in our lab. Figure 5 demonstrates the wide dose window of HIBL; 12 nm

half-pitch nested L's can be clearly patterned by a dose ranging from 120 to 320 pC/cm. This relatively large process window benefits the patterning of high-resolution features over large areas for device and mask fabrication.

#### IV. SUMMARY

We demonstrated 4 nm lithography resolution using a scanning focused helium ion beam in HSQ resist. Using the HSQ patterns as a nanoimprint template, we combined helium ion beam patterning with nanoimprint lithography using a UV-curable resist to demonstrate 4 nm half-pitch patterning resolution for a potentially high-throughput, single-digit nanometer fabrication process.

#### ACKNOWLEDGMENTS

W.D.L. acknowledges partial financial support from the Seed Funding Program for Basic Research from the University of Hong Kong (201203159015). The authors thank Dr. Bill Thompson for helpful discussion. We also thank Dr. John Paul Strachan, Tan Ha, and Cuong Le for experimental help and equipment maintenance.

- <sup>1</sup>G. E. Moore, *Electronics* **38**, 4 (1965).
- <sup>2</sup>J. K. W. Yang, B. Cord, H. Duan, K. K. Berggren, J. Klingfus, S.-W. Nam, K.-B. Kim, and M. J. Rooks, *J. Vac. Sci. Technol. B* **27**, 2622 (2009).
- <sup>3</sup>B. Cord, J. Yang, H. Duan, D. C. Joy, J. Klingfus, and K. K. Berggren, *J. Vac. Sci. Technol. B* **27**, 2616 (2009).
- <sup>4</sup>B. W. Ward, J. A. Notte, and N. P. Economou, *J. Vac. Sci. Technol. B* **24**, 2871 (2006).
- <sup>5</sup>D. Winston *et al.*, *J. Vac. Sci. Technol. B* **27**, 2702 (2009).
- <sup>6</sup>V. Sidorkin, E. van Veldhoven, E. van der Drift, P. Alkemade, H. Salemink, and D. Maas, *J. Vac. Sci. Technol. B* **27**, L18 (2009).
- <sup>7</sup>L. Scipioni, C. A. Sanford, J. Notte, B. Thompson, and S. McVey, *J. Vac. Sci. Technol. B* **27**, 3250 (2009).
- <sup>8</sup>M. C. Lemme, D. C. Bell, J. R. Williams, L. A. Stern, B. W. H. Baugher, P. Parillo-Herrero, and C. M. Marcus, *ACS Nano* **3**, 2674 (2009).
- <sup>9</sup>D. C. Bell, M. C. Lemme, L. A. Stern, J. R. Williams, and C. M. Marcus, *Nanotechnology* **20**, 455301 (2009).
- <sup>10</sup>D. Bazou, G. Behan, C. Reid, J. J. Boland, and H. Z. Zhang, *J. Microsc.* **242**, 290 (2011).
- <sup>11</sup>R. Hill, J. A. Notte, and L. Scipioni, *Advances in Imaging and Electron Physics* (Academic, New York, 2012), Vol. 170, Chap. 2.
- <sup>12</sup>R. Livengood, S. Tan, Y. Greenzweig, J. Notte, and S. McVey, *J. Vac. Sci. Technol. B* **27**, 3244 (2009).
- <sup>13</sup>S. Y. Chou, P. R. Krauss, and P. J. Renstrom, *J. Vac. Sci. Technol. B* **14**, 4129 (1996).
- <sup>14</sup>W. Wu *et al.*, *Nano Lett.* **8**, 3865 (2008).
- <sup>15</sup>F. Hua *et al.*, *Nano Lett.* **4**, 2467 (2004).
- <sup>16</sup>M. D. Austin, H. X. Ge, W. Wu, M. T. Li, Z. N. Yu, D. Wasserman, S. A. Lyon, and S. Y. Chou, *Appl. Phys. Lett.* **84**, 5299 (2004).
- <sup>17</sup>J. K. W. Yang and K. K. Berggren, *J. Vac. Sci. Technol. B* **25**, 2025 (2007).
- <sup>18</sup>D. Morecroft, J. K. W. Yang, S. Schuster, K. K. Berggren, Q. F. Xia, W. Wu, and R. S. Williams, *J. Vac. Sci. Technol. B* **27**, 2837 (2009).
- <sup>19</sup>G. Y. Jung, Z. Y. Li, W. Wu, Y. Chen, D. L. Olynick, S. Y. Wang, W. M. Tong, and R. S. Williams, *Langmuir* **21**, 1158 (2005).
- <sup>20</sup>Z. W. Li *et al.*, *Nano Lett.* **9**, 2306 (2009).
- <sup>21</sup>D. Drouin, A. R. Couture, D. Joly, X. Tastet, V. Aimez, and R. Gauvin, *Scanning* **29**, 92 (2007).
- <sup>22</sup>J. F. Ziegler, M. D. Ziegler, and J. P. Biersack, *Nucl. Instrum. Meth. B* **268**, 1818 (2010).
- <sup>23</sup>D. Winston, J. Ferrera, L. Battistella, A. E. Vladar, and K. K. Berggren, *Scanning* **34**, 121 (2012).